



PAPER • OPEN ACCESS

Marine seaweed *Sargassum wightii* extract as a low-cost sensitizer for ZnO photoanode based dye-sensitized solar cell

To cite this article: Muthusamy Anand and Santhanakrishnan Suresh 2015 *Adv. Nat. Sci: Nanosci. Nanotechnol.* **6** 035008

View the [article online](#) for updates and enhancements.

You may also like

- [Brown algae invasions and bloom events need routine monitoring for effective adaptation](#)
Victoria Dominguez Almela, Emma L. Tompkins, Jadu Dash et al.
- [Nutritional composition and alginate characteristics of *Sargassum polycystum* \(C. Agardh, 1824\) growth in Sebesi island coastal, Lampung-Indonesia](#)
I K Sumandiarsa, D G Bengen, J Santoso et al.
- [Effect of the ratio *Limncharis* sp. and *Sargassum* sp. on the characteristics of seaweed salt](#)
Nurjanah, A Abdullah, A M Jacob et al.

Marine seaweed *Sargassum wightii* extract as a low-cost sensitizer for ZnO photoanode based dye-sensitized solar cell

Muthusamy Anand and Santhanakrishnan Suresh

Department of Marine and Coastal Studies, School of Energy, Environment and Natural Resources, Madurai Kamaraj University, Madurai 625 021, Tamil Nadu, India

E-mail: anandm21@yahoo.com

Received 13 February 2015

Accepted for publication 20 April 2015

Published 15 May 2015



Abstract

The exploitation of marine seaweed (*Sargassum wightii*) extract as a low-cost sensitizer for a ZnO photoanode based solar cell is reported. The UV-vis absorbance spectrum of the *Sargassum wightii* (*S. wightii*) extract has exhibited three absorption peaks at 412.5, 610 and 659.5 nm in visible region of the solar spectrum. The pigment analysis has confirmed the presence of photosynthetic pigments such as chlorophylls, carotenoids and fucoxanthin. The photovoltaic performance of the *S. wightii* extract as a sensitizer in ZnO photoanode based solar cell is examined under simulated solar light irradiation. The solar cell sensitized with the *S. wightii* extract has delivered a short-circuit photocurrent density (J_{sc}) of $203 \mu A cm^{-2}$, open-circuit photo-voltage (V_{oc}) of 0.33 V, maximum peak power (P_{max}) of $31.02 \mu W$, fill factor of 0.46 and an overall solar to electrical energy conversion efficiency (η) of 0.07%. The sustainability of the solar cell is demonstrated through stability study. The overall results of this study suggest that the exploration of vast marine seaweed pigment resources and their use as sensitizer in solar cell would be a low-cost and environment friendly alternative to the expensive ruthenium metal complexes.

Keywords: dye-sensitized solar cell, marine seaweed, *Sargassum wightii*, natural sensitizer, photovoltaic performance

Classification numbers: 2.02, 4.02

1. Introduction

The population growth, rapid use of fossil fuels and related serious climate change issues have stimulated the search for an efficient, sustainable and eco-friendly renewable energy resource [1, 2]. The conversion of sunlight into electricity with the aid of low-cost photovoltaic technology is an active and contemporary research area, being devoted to overcome the global energy demand and environmental problems [3]. Since the first efficient dye-sensitized solar cell (DSSC) discovery in 1991, the research interest on DSSC has rapidly developed due to its efficiency, low-cost, simple fabrication technology, multi-color option, short energy payback period and flexibility [4–7]. The outcome of scientific reports about DSSC is remarkable because of active research efforts to improve the efficiency of DSSC by

modifying its existing components or by introducing new materials [8].

Among the basic components of DSSC, the dye sensitizer is regarded as most crucial since the performance of DSSC mainly depends on the absorption feature of the sensitizer, its charge carrier generation ability and adsorption tendency towards semiconductor surface [9]. The most commonly used sensitizers are ruthenium metal complexes because of their broad absorption in the visible region of the solar spectrum, metal-to-ligand charge transfer property and better attachment to the semiconductor surface [10, 11]. However, the drawbacks associated with the ruthenium metal complexes such as least availability of expensive ruthenium metal and low molar extinction coefficient are the major hurdles towards their application in DSSC [12]. In this respect, metal-free organic dyes with reliable performance





Figure 1. Photograph of *Sargassum wightii* seaweed collected from the Gulf of Mannar Region, Southeast Coast of India, Tamil Nadu.

have gained significant attention as potential alternatives to the proficient ruthenium metal complexes due to their high molar extinction coefficient, simple synthesis and low-cost [13–16]. Meanwhile, the natural pigments such as anthocyanin, chlorophylls, tannin and carotene present in plant parts (leaves, flowers, fruits, roots and barks) have also been increasingly investigated as organic sensitizers because of their more striking benefits, including low-cost, easy availability, abundance in raw materials and absence of environment threat compared to synthetic organic and inorganic dyes [17–22]. Recently, the interest on marine seaweeds has also gained attention, owing to the fact that the abundant photosynthetic pigments present in the seaweeds could be employed as alternative sensitizers [23, 24]. The seaweeds contain major photosynthetic pigments such as c-type chlorophylls, including chlorophyll c_1 and chlorophyll c_2 , usually have carboxyl groups in their terminals, connected to the porphyrin macrocycle through a conjugated double bond. This facilitates the seaweed pigments to potentially inject photogenerated electrons from the porphyrin macrocycle to semiconductor electrode surface on which the seaweed pigments anchored [23].

Nanocrystalline titanium dioxide (TiO_2) is the widely employed photoanode material in DSSC due to its high surface area. However, equal importance is paid to nanocrystalline zinc oxide (ZnO), because of its similar wide band-gap energy and physical properties as that of TiO_2 . The major advantage of using ZnO as photoanode material in DSSC is its higher electron transport property, which reduces undesired charge recombination that takes place between conduction band electrons of the semiconductor photoanode and oxidized dye molecules/triiodide ions in the electrolyte. The ZnO photoanode based solar cells sensitized by metal-free organic dyes with high molar extinction coefficient and favorable surface attachment groups have exhibited good photovoltaic performance [25, 26]. In light of the above facts, in the present work, we have studied the photovoltaic performance of a marine seaweed, *Sargassum wightii* (*S. wightii*) extract in a solar cell. The *S. wightii* seaweed sample

(figure 1) was collected from the Gulf of Mannar Region, Southeast Coast of India, Tamil Nadu. The seaweed extract was characterized by UV–vis spectrophotometry and Fourier transform infrared (FTIR) spectroscopy. The photovoltaic performance of the *S. wightii* extract was evaluated by employing it as sensitizer for a ZnO nanoparticles (ZnO NPs) photoanode based solar cell and the results are discussed. The scheme for the solar cell sensitized by marine seaweed *S. wightii* extract is shown in figure 2.

2. Experimental details

2.1. Chemical reagents

The marine seaweed, *S. wightii* was collected from the Pudhumadam coast of Gulf of Mannar, Southeast coast of India, Tamil Nadu. Chemical reagents, such as high pure zinc acetate dihydrate and oxalic acid dihydrate were procured from Merck. Highly stable imidazole based liquid electrolyte (EL-HSC) was supplied by Dyesol, Australia. Fluorine-doped tin oxide (FTO) conducting glass (TEC-7, sheet resistance = $\sim 6\text{--}8\ \Omega\ \text{cm}^{-2}$) was obtained from Pilkington, Mumbai, India. All other chemicals used in this work were of analytical grade. Unless otherwise specified, deionized double distilled water was used for the preparation of aqueous solutions and washings.

2.2. Preparation of *S. wightii* seaweed extract

The *S. wightii* seaweed sample was washed with fresh water several times to remove salts and finally washed with distilled water couple of times. The washed seaweed sample was shade dried to remove moisture content completely. The dried sample was ground in a mixer grinder to get a seaweed powder. Around 1 g of the seaweed powder was soaked in 60 mL of absolute ethanol and kept in a refrigerator for 24 h. The ethanolic solution of *S. wightii* seaweed extract was used for further studies.

2.3. Synthesis of ZnO NPs

The ZnO NPs were synthesized by following the previously reported procedure [27]. In brief, equal volume of zinc acetate dihydrate (0.1 M) and oxalic acid dihydrate (0.1 M) aqueous solutions were mixed together by stirring for 12 h at room temperature. The obtained white precipitate was filtered, washed sequentially with acetone and distilled water several times to remove impurities. Then, the precipitate was dried in a vacuum oven at $120\ ^\circ\text{C}$ for 6 h to remove water molecules completely. Finally, the formed ZnO NPs were calcinated at $450\ ^\circ\text{C}$ for 2 h in a muffle furnace.

2.4. Characterization studies

Absorption spectrum of *S. wightii* seaweed extract was recorded in a UV–vis spectrophotometer (UV-2550, Shimadzu). FTIR spectrum was recorded in the region between 4000 and $400\ \text{cm}^{-1}$ using a Shimadzu FTIR spectrometer

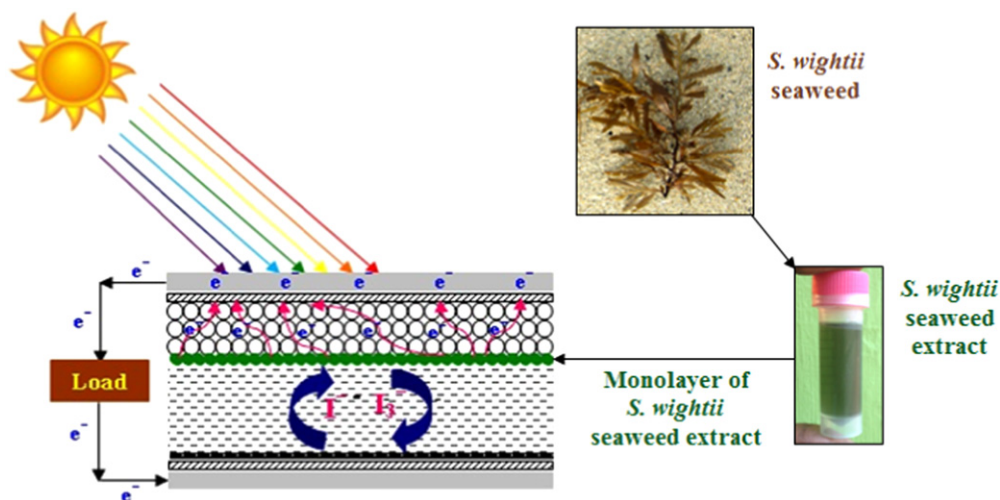


Figure 2. Scheme for the solar cell sensitized by marine seaweed *Sargassum wightii* extract.

(Model 8400S). The pigments present in the ethanol extract of *S. wightii* seaweed were analyzed according to the previous reports [28–31]. Scanning electron microscopy (SEM) images of the ZnO NPs were taken in a VEGA 3 TESCAN SEM instrument. Elemental composition of the ZnO NPs was subsequently analyzed after the SEM analysis by using the same instrument. Oriel class-A solar simulator (M-91195A, Newport) containing ozone-free 450 W xenon lamp was used as a light source for testing the solar cell. A computer-controlled Autolab PGSTAT302N electrochemical workstation was employed for photocurrent–voltage (I – V) and photocurrent–time (I – T) measurements.

2.5. Fabrication of DSSC and its performance evaluation

1 g of the synthesized ZnO NPs were ground in a porcelain mortar with 0.35 mL of distilled water and 33.5 μ L of acetylacetone until get a viscous paste. Then, 1.35 mL of distilled water was gradually added under continuous grinding followed by the addition of 15 μ L triton X-100. The obtained paste was used to form a thin film on conducting side of a FTO glass with an active surface area of 1 cm² [32]. The addition of acetylacetone prevents reaggregation of ZnO NPs and triton X-100 facilitates spreading of ZnO colloidal paste on the surface of FTO conducting glass. The thin film was dried in air for 15 min, kept at 400 °C in a muffle furnace for 5 min and the same procedure was repeated three times to get an optimum thick (\sim 10 μ m) film. Then, the film was calcinated at 450 °C for 30 min and allowed to cool down to 80 °C. The hot film at 80 °C was immersed in ethanolic solution of *S. wightii* seaweed extract and kept in a refrigerator for 24 h. The dye-adsorbed ZnO photoanode was withdrawn from the ethanolic extract solution under a stream of nitrogen gas which was immediately sandwiched with the platinum deposited counter electrode by using alligator clips. The platinum counter electrode was prepared on FTO conducting glass substrates using 7×10^{-3} M $\text{H}_2\text{PtCl}_6 \cdot 6\text{H}_2\text{O}$ solution in 2-propanol, where Pt^{4+} ions were thermally reduced at 400 °C. Finally, few drops of imidazole based

liquid electrolyte was dropped sideways in the gap between the two electrodes through which the electrolyte was occupied the space between them with an aid of surface tension. The fill factor (FF) and efficiency (η) of the DSSC was evaluated by using the following equations:

$$\text{FF} = \frac{I_{\text{max}} V_{\text{max}}}{I_{\text{sc}} V_{\text{oc}}},$$

$$\eta(\%) = \frac{I_{\text{sc}} V_{\text{oc}} \text{FF}}{P_{\text{in}}} \times 100,$$

where I_{sc} is the short-circuit photocurrent, V_{oc} is the open-circuit photovoltage, P_{in} is the power of incident light (45 mW cm⁻²), I_{max} and V_{max} are the photocurrent and photovoltage delivered at maximum power point, respectively.

3. Results and discussion

3.1. UV–vis absorption analysis of *S. wightii* extract

The UV–vis absorption spectrum was recorded to elucidate the potency of *S. wightii* seaweed extract to be used as a sensitizer in solar cell. The UV–vis absorption spectrum of the *S. wightii* seaweed extract is shown in figure 3(a) and its transmittance spectrum is given in figure 3(b). One of the essential requirements for a best performing sensitizer is broad and intense absorption in the visible and near-IR region of the solar spectrum [33]. The absorption spectrum of the *S. wightii* seaweed extract showed a broad absorbance in the wavelength range between 300 and 700 nm, with absorption peaks at 412.5, 610 and 659.5 nm in visible region of the solar spectrum. These absorption peaks can be associated with the characteristic absorption of chlorophylls [34, 35].

Generally, the chlorophylls exhibit strong absorption in the blue and red regions of the solar spectrum. However, they show poor absorption in the green region, which is consistent with our result. The absorption wavelength of each peak and their intensity exhibited by the *S. wightii* seaweed extract can

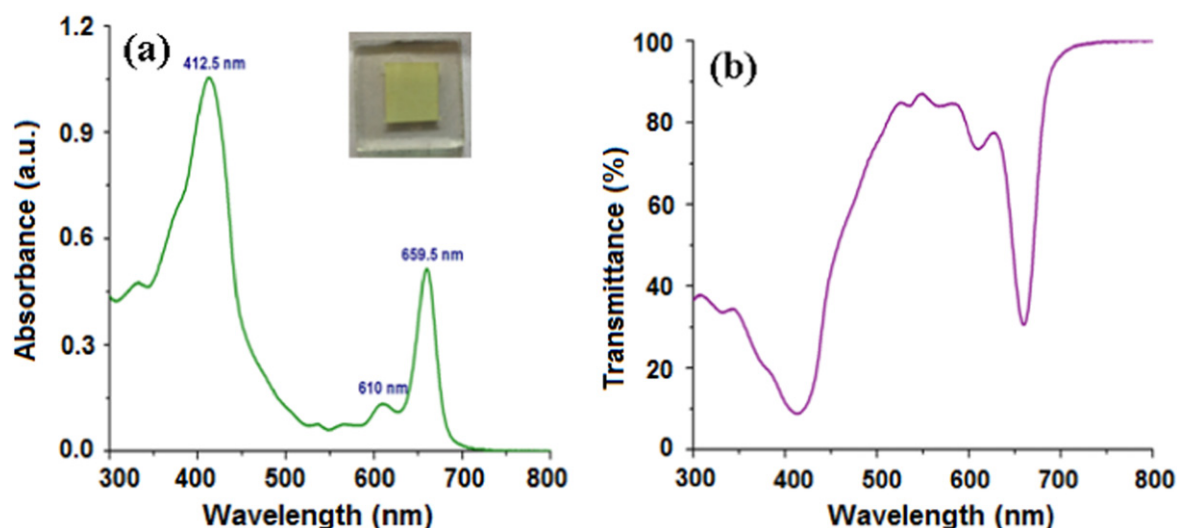


Figure 3. UV-vis absorption (a) and transmittance (b) spectra of *S. wightii* extract in ethanol. Inset of figure 3(a) shows the *S. wightii* extract adsorbed ZnO nanoparticles thin film photoanode.

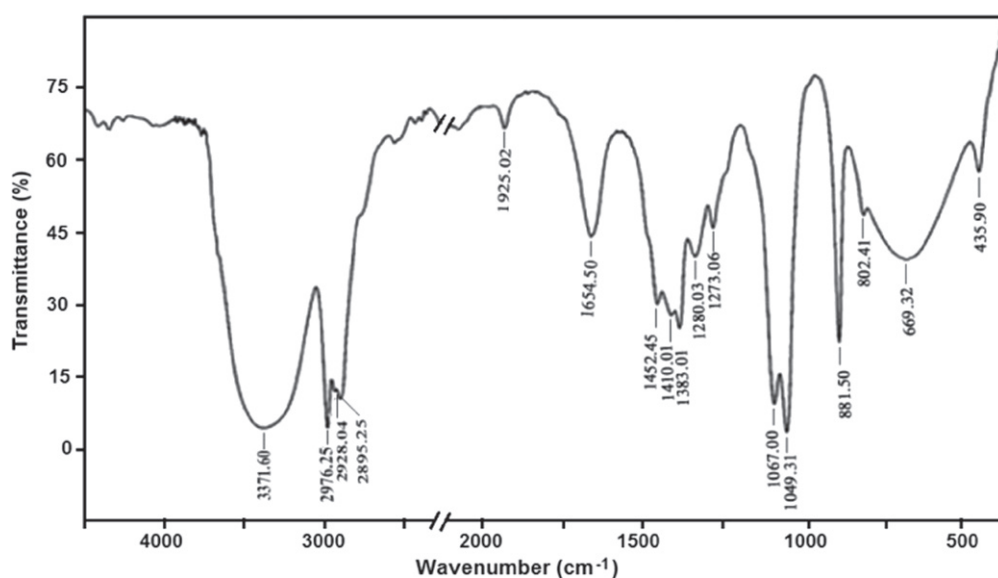


Figure 4. FTIR spectrum of *S. wightii* seaweed extract.

be ascribed to the transition energies and transition-dipole moments in transition from ground state to the Soret, Q_x and Q_y singlet-excited states [24]. The broad absorption of *S. wightii* seaweed extract in the visible region can result in absorption of higher photon energy which leads to generate more photoelectrons. Moreover, this broad absorption can facilitate a higher number of delocalized π -electrons in the molecular system for the improved photocurrent generation [36].

3.2. FTIR analysis of *S. wightii* extract

FTIR spectroscopy can be employed for the qualitative determination of organic constituents and functional groups present in plant and seaweed species and hence, the FTIR spectrum of *S. wightii* extract was recorded (figure 4). The absorption bands situated in the region between 1100 and

1000 cm^{-1} are corresponding to the C-H bending or C-O or C-C stretching vibrations of carbohydrates [37] and polysaccharides [38] present in the *S. wightii* extract. The band observed around 881 cm^{-1} is due to the aromatic C-H out-of-plane vibration, which indicates the existence of aromatic ring pigment compound [39]. The weak absorption band centered at 669 cm^{-1} can be ascribed to the C-H bending vibration, which is also confirmed the presence of carbohydrates. The strong and broad absorption band positioned at 3371 cm^{-1} can be attributed to the free O-H and N-H stretching vibrations of the amino acids [40]. The existence of chlorophyll groups are confirmed through the C-H stretching vibrations at 2976, 2928 and 2895 cm^{-1} [41]. The weak absorption bands observed between 2344 and 2365 cm^{-1} correspond to the C-O stretching which are the characteristic peaks of carboxylic group [42]. The absorption band centered at 1654 cm^{-1} is due to the C-O stretching and N-O asymmetric

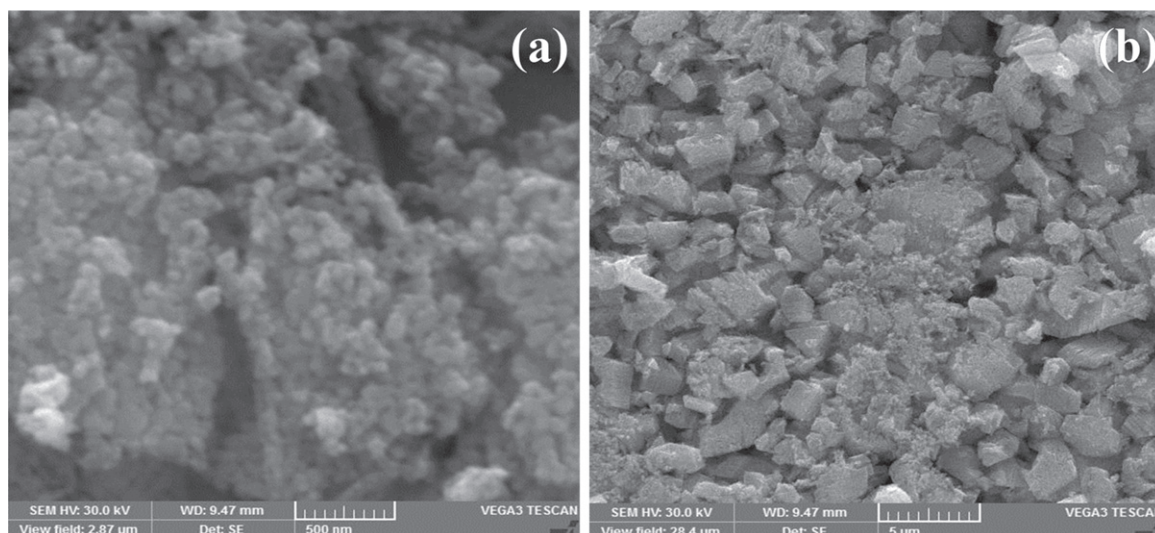


Figure 5. SEM images of ZnO NPs (a) higher magnified image and (b) lower magnified image.

stretching of the ester group [43]. The bands around 1452 and 1410 cm^{-1} are due to the C–C stretching vibration of aromatic ring compound. The medium absorption band at 1273 cm^{-1} is indicating the C–N stretching vibration of chlorophyll. The FTIR results suggest that carbohydrate and chlorophyll are the major constituents of the *S. wightii* seaweed extract.

3.3. SEM and EDX analysis of ZnO NPs

The SEM images of ZnO NPs were recorded and are shown in figure 5. It is obvious that particle size and surface potential of the semiconductor nanoparticles could control the amount of dye adsorbed on their surface that determines the number of photogenerated charge carriers generation and hence overall efficiency of the DSSC [44]. The higher magnified SEM image clearly exhibits the presence of spherical and uniform ZnO NPs with size range between 40 and 50 nm (figure 5(a)). The ZnO NPs consist of clusters of small grains. The ZnO NPs are highly interconnected with each other which could facilitate fast diffusion of photogenerated electrons and considerable voids between the nanoparticles could favor the better interfacial charge transfer. The lower magnified SEM image shows the presence of coarse ZnO nanostructures with undefined morphology, which are made up of combination of several spherical ZnO NPs (figure 5(b)). The EDX analysis was subsequently performed during SEM analysis (figure 6). The EDX spectrum clearly discloses the existence of Zn and O elements alone. The absence of any other impurities in the EDX spectrum reveals that ZnO only formed through our synthesis procedure.

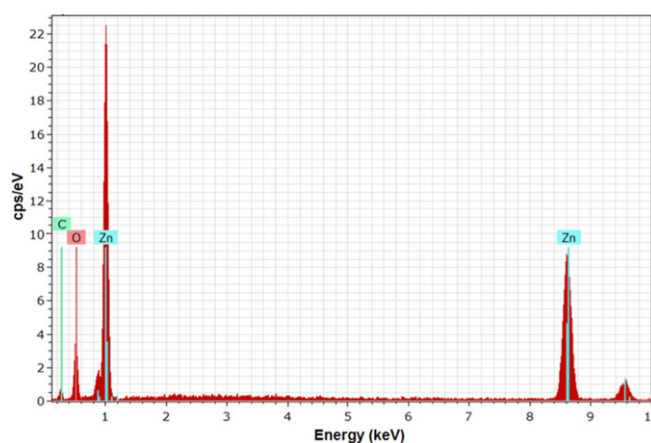


Figure 6. EDX spectrum of ZnO NPs.

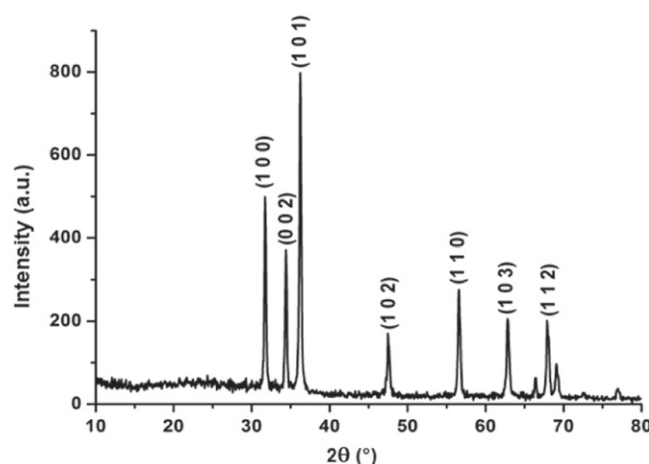


Figure 7. XRD pattern of ZnO NPs calcinated at $450\text{ }^{\circ}\text{C}$.

3.4. X-ray diffraction (XRD) analysis of ZnO NPs

The purity and crystalline nature of the ZnO NPs were analyzed through powder XRD analysis (figure 7).

The ZnO sample must be annealed to improve its crystallinity and hence the ZnO sample was calcinated in a muffle furnace under oxygen atmosphere. The typical furnace

annealing was carried out at $450\text{ }^{\circ}\text{C}$ to improve the characteristics of ZnO sample. The well resolved diffraction peaks noticed at 2θ values of 31.7 , 34.4 , 36.4 , 47.5 , 57.1 , 63.2 , 66.7 , 67.8 , 69 , 72.6 and 76.8° are matched well those to Bragg's

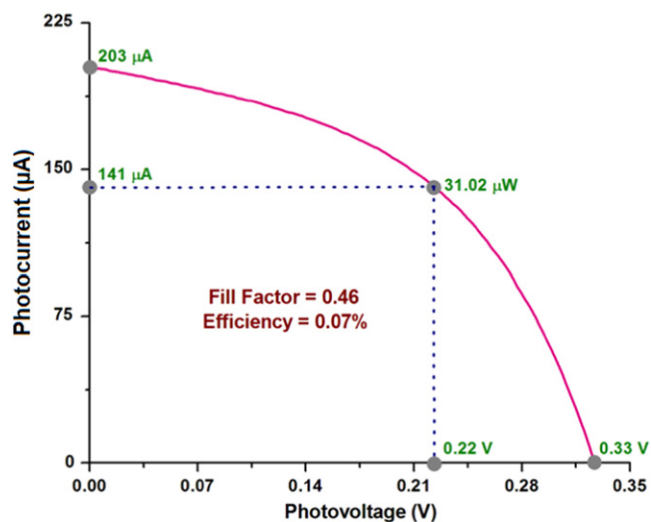


Figure 8. Photocurrent–photovoltage (I – V) characteristics of DSSC sensitized with *S. wightii* seaweed extract.

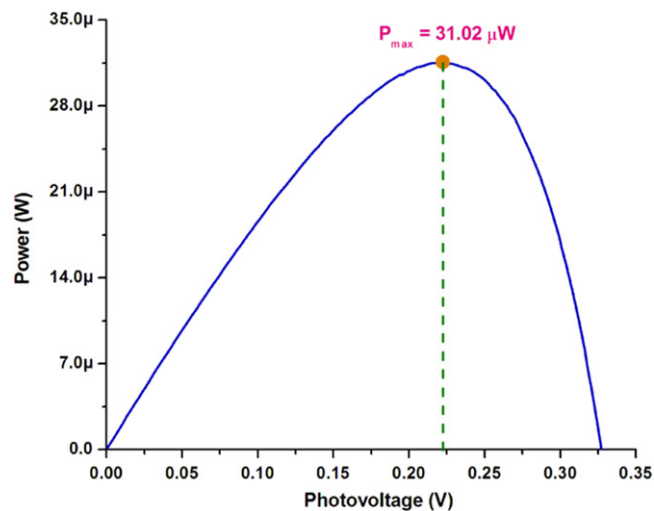


Figure 9. Power curve of DSSC sensitized with *S. wightii* seaweed extract.

reflection of the standard wurtzite structure hexagonal ZnO with lattice constants a and c of 3.25 and 5.20 Å, respectively (JCPDS file no. 36-1451). The observed diffraction plane (0 0 2) intensity is corresponding to 2θ value of 34.4° and its diffraction planes intensity ratio ($R_{(002)/(101)}$) value is 0.44, which suggests that the formed ZnO NPs are hexagonal in shape [45]. The diffraction peaks of the annealed samples become more intense and sharper and this discloses that the crystal quality of ZnO has improved as a consequence of high temperature annealing. The full width at half maximum of ZnO sample has decreased while increasing the temperature.

3.5. Photocurrent–photovoltage (I – V) characteristics of DSSC

The photocurrent–photovoltage (I – V) curve of the solar cell sensitized with *S. wightii* seaweed extract is given in figure 8 and its corresponding power curve is shown in figure 9. The short-circuit photocurrent and open-circuit photovoltage are the most crucial parameters, which decide the efficiency of the cell. In our case, the solar cell sensitized with *S. wightii* seaweed extract exhibited a short-circuit photocurrent density (J_{sc}) of $203 \mu\text{A cm}^{-2}$, open-circuit photovoltage (V_{oc}) of 0.33 V, maximum peak power (P_{max}) of $31.02 \mu\text{W}$, FF of 0.46 and an overall solar to electrical energy conversion efficiency (η) of 0.07%. Generally, the natural dyes employed as sensitizers in solar cell deliver very low efficiencies when compared to synthetic organic and inorganic dyes, due to the absence of specific functional attachment groups and low absorption in the visible region of the solar spectrum [8]. The significant photocurrent generated in our work can be ascribed to the broad absorption of the *S. wightii* seaweed extract in visible region of the solar spectrum, owing to the presence of basic photosynthetic pigments. The pigment analysis of the *S. wightii* seaweed extract showed the presence of chlorophyll a (0.16 mg g^{-1}), chlorophyll b (0.19 mg g^{-1}), chlorophyll c_1 and c_2 (0.17 mg g^{-1}), carotenoids (0.003 mg g^{-1}) and fucoxanthin (0.036 mg g^{-1}). These pigments effectively capture the incoming photons and generate higher number of

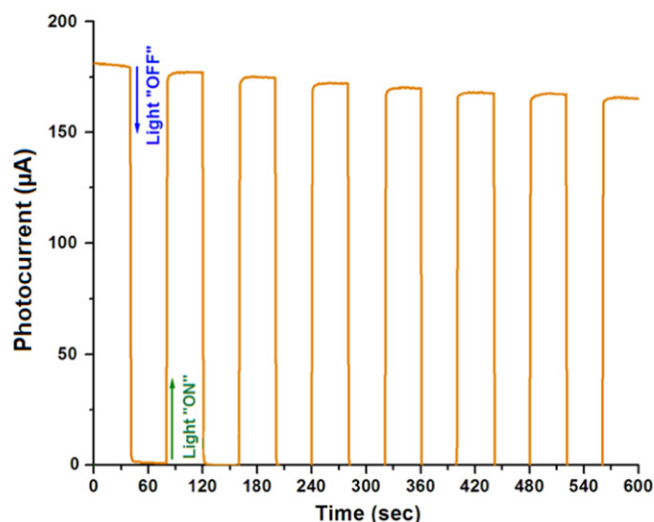
photogenerated electrons, which lead to the significant current production in the DSSC. In terms of ZnO NPs photoanode, the photovoltaic parameters obtained in our work can be comparable with the previous reports [24, 46] of TiO_2 photoanode based DSSCs sensitized with seaweed and green algae extracts (table 1). Therefore, the use of seaweed photosynthetic pigments as sensitizers in solar cell could be an appropriate solution for the production of low-cost DSSCs by eliminating the high-cost ruthenium metal complexes. Moreover, the exploitation of seaweeds for energy conversion through solar cell would facilitate transformation of natural seaweed resources into valuable biomass. Further optimization studies and ways to improve the efficiency of the present DSSC are under progress.

3.6. Transient photocurrent–time (I – T) profile of DSSC

The stability and photocurrent generation nature of the solar cell sensitized with *S. wightii* seaweed extract were analyzed by chronoamperometry technique for a total time of 600 s and the obtained transient photocurrent–time (I – T) profile is shown in figure 10. The transient photocurrent–time profile observed for the DSSC is well accordance with its corresponding I – V profile character. During the chronoamperometry experiment, when the light in the solar simulator was switched ‘ON’ to illuminate the solar cell, a sharp rise in the photocurrent was observed. When the light was switched ‘OFF’ after a specified time interval of 40 s by closing the mechanical shutter in the solar simulator, the photocurrent was suddenly dropped down to zero. It can be inferred from these results that the dye regeneration of oxidized dye was fast enough to keep pace with the charge carrier injection rate from the excited dye molecules. The highest photocurrent observed was almost remained the same in the absence of any considerable decay after several ‘ON–OFF’ cycles during the whole period of light illumination, which reveals good stability of the solar cell. Moreover, the stability test indicates good stability of the *S. wightii* seaweed

Table 1. Photovoltaic parameters of solar cells sensitized with different seaweeds and green algae extracts.

Sensitizer	Photoanode material	J_{sc} ($\mu A\ cm^{-2}$)	V_{oc} (V)	FF	η (%)	Reference
<i>S. wightii</i> seaweed extract	ZnO NPs	203	0.33	0.46	0.07	Present work
Green algae extract	TiO ₂ NPs	397	0.56	0.44	0.10	[46]
<i>U. pinnatifida</i> seaweed extract	TiO ₂ NPs	800	0.36	0.69	0.18	[24]

**Figure 10.** Photocurrent–time (I – T) profile of DSSC sensitized with *S. wightii* seaweed extract.

extract as sensitizer over the ZnO NPs thin film photoanode and hence it can be used as a stable sensitizer for DSSC.

4. Summary

The marine seaweed, *Sargassum wightii* extract was used as a low-cost sensitizer for ZnO NPs photoanode based solar cell. The UV–vis absorbance spectrum of the *S. wightii* extract showed three absorption peaks at 412.5, 610 and 659.5 nm in visible region of the solar spectrum. The FTIR spectrum revealed the presence of carbohydrate and chlorophylls in the *S. wightii* extract and its pigment analysis confirmed the existence of photosynthetic pigments such as chlorophylls, carotenoids and fucoxanthin. The photovoltaic performance of the *S. wightii* extract as sensitizer in a ZnO NPs photoanode based solar cell was evaluated under simulated solar light irradiation. The solar cell sensitized with *S. wightii* extract delivered a short-circuit photocurrent density (J_{sc}) of $203\ \mu A\ cm^{-2}$, open-circuit photovoltage (V_{oc}) of 0.33 V, FF of 0.46 and an overall solar to electrical energy conversion efficiency (η) of 0.07%. The stability test of the solar cell sensitized with *S. wightii* seaweed extract disclosed consistency in the photocurrent production for a light irradiation period of 600 s. The overall results of the study suggest that the exploitation of marine seaweed pigments as natural sensitizer could be a possible alternative for the production of low-cost and environment friendly DSSCs.

Acknowledgments

The authors acknowledge the Scientific and Engineering Research Board (SERB), New Delhi, Government of India for financial support (SB/EMEQ-061/2013) under ‘Empowerment and Equity Opportunities for Excellence in Science’ programme. The authors express their thanks to the University with Potential for Excellence (UPE) Scheme, Madurai Kamaraj University for providing instrumentation facility. The authors are grateful to M/s Dyesol, Australia and M/s Pilkington, Mumbai, India for generously providing highly stable imidazole based liquid electrolyte (EL-HSC) and TEC-7 FTO conducting glass, respectively for research purpose.

References

- [1] Armaroli N and Balzani V 2007 *Angew. Chem., Int. Ed. Engl.* **46** 52
- [2] Ørnsø K B, Garcia-Lastra J M and Thygesen K S 2013 *Phys. Chem. Chem. Phys.* **15** 19478
- [3] Sista S, Hong Z, Chen L M and Yang Y 2011 *Energy Environ. Sci.* **4** 1606
- [4] O'Regan B and Grätzel M 1991 *Nature* **353** 737
- [5] Yella A, Lee H W, Tsao H N, Yi C, Chandiran A K, Nazeeruddin M K, Diau E W G, Yeh C Y, Zakeeruddin S M and Grätzel M 2011 *Science* **334** 629
- [6] Daenke T, Kwon T H, Holmes A B, Duffy N W, Bach U and Spiccia L 2011 *Nat. Chem.* **3** 211
- [7] Gonçalves L M, de Zea Bermudez V, Ribeiro H A and Mendes A M 2008 *Energy Environ. Sci.* **1** 655
- [8] Hagfeldt A, Boschloo G, Sun L, Kloo L and Pettersson H 2010 *Chem. Rev.* **110** 6595
- [9] Tennakone K, Kumara G R R A, Kumarasinghe A R, Sirimanne P M and Wijayantha K G U 1996 *J. Photochem. Photobiol. A* **94** 217
- [10] Wang P, Zakeeruddin S M, Moser J E, Humphry-Baker R, Comte P, Aranyos V, Hagfeldt A, Nazeeruddin M K and Grätzel M 2004 *Adv. Mater.* **16** 1806
- [11] Robertson N 2006 *Angew. Chem., Int. Ed. Engl.* **45** 2338
- [12] Kanaparthi R K, Kandhadi J and Giribabu L 2012 *Tetrahedron* **68** 8383
- [13] Ito S *et al* 2006 *Adv. Mater.* **18** 1202
- [14] Kuang D, Uchida S, Humphry-Baker R, Zakeeruddin S M and Grätzel M 2008 *Angew. Chem., Int. Ed. Engl.* **47** 1923
- [15] Mishra A, Fischer M K R and Bauerle P 2009 *Angew. Chem., Int. Ed. Engl.* **48** 2474
- [16] Suresh S, Pandikumar A, Murugesan S, Ramaraj R and Raj S P 2011 *Mater. Express* **1** 307
- [17] Kumara G R A, Kaneko S, Okuya M, Onwona-Agyeman B, Konno A and Tennakone K 2006 *Sol. Energ. Mat. Sol. Cells* **90** 1220
- [18] Zhang D, Lanier S M, Downing J A, Avent J L, Lum J and McHale J L 2008 *J. Photochem. Photobiol. A* **195** 72
- [19] Ito S, Saitou T, Imahori H, Uehara H and Hasegawa N 2010 *Energy Environ. Sci.* **3** 905

- [20] Narayan M R 2012 *Renew. Sustain. Energy Rev.* **16** 208
- [21] Shanmugam V, Manoharan S, Anandan S and Murugan R 2013 *Spectrochim. Acta A* **104** 35
- [22] Singh L K, Karlo T and Pandey A 2014 *Spectrochim. Acta A* **118** 938
- [23] Wang X F, Zhan C H, Maoka T, Wada Y and Koyama Y 2007 *Chem. Phys. Lett.* **447** 79
- [24] Calogero G, Citro I, Marco G D, Minicante S A, Morabito M and Genoves G 2014 *Spectrochim. Acta A* **117** 702
- [25] Yin X, Liu X, Wang L and Liu B 2010 *Electrochem. Commun.* **12** 1241
- [26] Cheng H M and Hsieh W F 2010 *Energy Environ. Sci.* **3** 442
- [27] Suresh S, Pandikumar A, Murugesan S, Ramaraj R and Raj S P 2011 *Sol. Energy* **85** 1787
- [28] Arnon D I 1949 *Plant Physiol.* **24** 1
- [29] Jeffrey S W 1961 *Biochem. J.* **80** 336
- [30] Jensen A and Jensen S L 1959 *Acta Chem. Scand.* **13** 1863
- [31] Seely G R, Duncan M J and Vidaver W E 1972 *Mar. Biol.* **12** 184
- [32] Nazeeruddin M K, Kay A, Rodicio I, Humphry-Baker R, Mueller E, Liska P, Vlachopoulos N and Grätzel M 1993 *J. Am. Chem. Soc.* **115** 6382
- [33] Nazeeruddin M K *et al* 2001 *J. Am. Chem. Soc.* **123** 1613
- [34] Lai W H, Su Y H, Teoh L G and Hon M H 2008 *J. Photochem. Photobiol. A* **195** 307
- [35] Kushwaha R, Srivastava P and Bahadur L 2013 *J. Energy* **654953** 1
- [36] Vinodgopal K, Hua X, Dalgren R L, Lappin A G, Patterson L K and Kamat P V 1995 *J. Phys. Chem.* **99** 10883
- [37] Li Y M, Sun S Q, Zhou Q, Qin Z, Tao J X, Wang J and Fang X 2004 *Vib. Spectrosc.* **36** 227
- [38] Nakamoto K 1986 *Infrared and Raman Spectra of Inorganic and Coordination Compounds* 4th edn (New York: Wiley)
- [39] Figueira M M, Volesky B and Mathieu H J 1999 *Environ. Sci. Technol.* **33** 1840
- [40] Rao C N R 1963 *Chemical Applications of Infrared Spectroscopy* (New York: Academic)
- [41] Socrates G 1994 *Infrared Characteristic Group Frequencies* (West Sussex, United Kingdom: Wiley)
- [42] Thirunavukkarasu R, Pandiyan P, Balaraman D, Subaramaniyan K, Jothi G E G, Manikkam S and Sadaiyappan B 2013 *J. Coast. Life Med.* **1** 26
- [43] Stewart D 1996 *Appl. Spectrosc.* **50** 357
- [44] Abdou E M, Hafez H S, Bakir E and Abdel-Mottaleb M S A 2013 *Spectrochim. Acta A* **115** 202
- [45] Raula M, Rashid M H, Paira T K, Dinda E and Mandal T K 2010 *Langmuir* **26** 8769
- [46] Taya S A, El-Agez T M, El-Ghamri H S and Abdel-Latif M S 2013 *Int. J. Mater. Sci. Appl.* **2** 37